NUMERICAL INVESTIGATION OF DEPTH RATIO EFFECTS ON THERMOHYDRAULIC PERFORMANCE OF A HEAT EXCHANGER WITH V-CUT TWISTED TAPE

Farrel Rizqiadinata[1], Damora Rhakasywi[2*], Nicky Yongkimandalan[3]
Mechanical Engineering Department, Faculty of Engineering, Universitas Pembangunan Nasional Veteran Jakarta, Jl. Limo Raya No.80, Limo, Kota Depok, Jawa Barat, 16514, Indonesia
E-mail: 2210311001@mahasiswa.upnvj.ac.id[1], rhakasywi@upnvj.ac.id[2]*, nickyyongkimandalan@upnvj.ac.id

Received	: 10 June 2026	Accepted	: 04 July 2026
Revised	: 22 June 2026	Published	: 27 July 2026

Abstract
Using Computational Fluid Dynamics (CFD), this research evaluates the thermo-hydraulic effects of altering the depth ratio of V-cut twisted tape (VTT) inserts within tubular heat exchangers. Three specific configurations (De/w = 0.25, 0.35, and 0.45) were simulated and compared to baseline cases of plain tubes and traditional twisted tapes. System characteristics were analyzed using flow behavior, Nusselt number, friction factor, and the Performance Evaluation Criterion (PEC). To ensure reliability, the numerical framework was verified using established empirical correlations and experimental data, yielding deviations below 5%. The simulated outcomes indicate that swirl generation, enhanced radial mixing, and thermal boundary-layer disruption drive the heat transfer improvements of the twisted tapes, with the V-cut geometries accelerating vortex generation and fluid recirculation. Although VTT systems successfully optimize thermal dissipation, they incur elevated hydraulic penalties. This trade-off between pressure drop and thermal efficiency is clearly reflected in the PEC trends, where flow visualizations confirm that larger depth ratios significantly augment fluid mixing and thermal restructuring.

Keywords: Computational Fluid Dynamic; Depth ratio; Heat exchanger; Twisted tape.

INTRODUCTION

The Energy-efficiency optimization in heat-exchanger systems has become a critical issue in modern industrial sectors. Industrial activities alone account for approximately 37% of global energy consumption and contribute nearly 18–20% of total carbon dioxide (CO_2) emissions worldwide (Hu & Man, 2023). In addition, a substantial amount of industrial waste heat remains underutilized despite its significant potential for energy recovery. Numerous studies have reported that waste-heat recovery through heat-exchanger technology can considerably improve overall system efficiency while simultaneously reducing energy losses in industrial processes (Turek et al., 2024)(Sulistiana et al., 2026). Therefore, the development of advanced heat-transfer enhancement technologies is essential to support sustainable energy utilization and carbon-emission reduction. One of the most widely applied approaches for improving heat-transfer performance is passive heat-transfer enhancement, which does not require additional external power and is relatively simple to implement in engineering applications (Thapa et al., 2021). Among the various passive enhancement techniques, twisted tape inserts have attracted considerable attention because of their ability to generate swirl flow, disrupt the thermal boundary layer, and intensify fluid turbulence (Hasan & Naji, 2023). This turbulence enhancement directly increases the Nusselt number (Nu), resulting in higher convective heat-transfer rates compared with plain tubes. However, the improvement in heat-transfer performance is generally accompanied by an increase in friction factor (f), which consequently leads to higher pressure drop and pumping-power consumption. Therefore, geometric optimization is required to achieve an appropriate balance between thermal enhancement and hydraulic penalty (Singh et al., 2022).

To overcome these limitations, various geometric modifications of twisted tapes have been developed, including perforated, dimpled, and edge-cut twisted tapes, aiming to enhance local turbulence while minimizing excessive flow resistance (Dagdevir & Ozceyhan, 2021)(Thote & Singh, 2023)(Diwaker & Kumar, 2023). Among these configurations, the V-cut twisted tape (VTT) has demonstrated promising thermo-hydraulic performance. The V-shaped cuts along the tape edges are capable of generating secondary vortices that intensify fluid mixing and strengthen the interaction between the working fluid and the tube wall (Diwaker & Kumar, 2023)(Nashee, 2024). Previous studies shows that this typical configuration does improves the performance of the heat-transfer compared with conventional twisted tapes, although the associated increase in pressure drop remains a major challenge in design optimization (Kumar et al., 2021). Despite these promising findings, most previous investigations have primarily focused on geometric variations based on absolute dimensions, making the results difficult to generalize for different heat-exchanger scales and operating conditions. In addition, there is a lack of extensive literature exploring how dimensionless geometric attributes, especially the depth ratio (De/w) affect thermo-hydraulic characteristics. This geometric ratio is critical in regulating secondary flow development, flow separation, and vortex strength, each of which fundamentally balances thermal dissipation improvements against hydraulic pressure losses. Nonetheless, prior research has predominantly concentrated on macroscopic thermal outputs, omitting a rigorous analysis of the foundational physics governing secondary vortex dynamics and swirl flow progression. Methodical efforts to map the depth ratio against turbulence profiles, flow structures, friction factors, Nusselt numbers, and the Performance Evaluation Criterion (PEC) are also uncommon. Utilizing normalized criteria like the depth ratio yields major benefits, such as broad versatility across diverse heat exchanger layouts, structural adaptability, and modular scaling. Consequently, an in-depth computational dissection is crucial to isolate the thermo-hydraulic impact of this geometric factor on V-cut twisted tape (VTT) channels, facilitating a structural design that achieves a balanced trade-off between pumping power demands and enhanced heat transfer. Addressing this gap, the present investigation leverages Computational Fluid Dynamics (CFD) to simulate the consequences of shifting depth ratios (De/w = 0.25, 0.35, and 0.45) on VTT configuration behavior. System efficacy is quantified using friction factors, Nusselt numbers, and the PEC to pinpoint the most thermally efficient and overall optimal design for tubular thermal management systems.

METHOD

Geometry Modeling

For this numerical model, the heat exchanger geometry was segregated into two primary computational fields: the fluid domain and the solid domain. The former encompasses the enclosed boundaries designated for fluid circulation, whereas the latter comprises a horizontal cylindrical tube measuring 1000 mm in length with a diameter of 17 mm. Inside the tube, the embedded twisted tape insert features a length of 1000 mm, a width of 16 mm, a material thickness of 1 mm, and a fixed twist ratio (y/w) of 5. To evaluate the V-cut twisted tape (VTT) design, the configuration was subjected to parametric variations across three distinct depth ratios (De/W), specifically 0.25, 0.35, and 0.45. Throughout these test cases, a uniform cut width of 4 mm and a pitch length of 80 mm were maintained. The comprehensive structural overview and dimension breakdown are illustrated in Figure 1 and tabulated in Table 1.

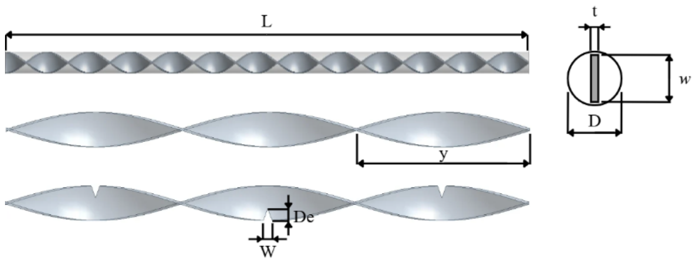

Figure 1. Geometry of pipe wih twisted tape insert

Table 1. Pipe and twisted tape spesification

Parameter	Symbol	Dimension (mm)
Tube Length	L	1000
Hydraulic Diameter	D	17
Twisted Tape Length	L	1000
Twisted Tape Thickness	t	1
Twisted Tape Wide	w	16
Twisted Tape Pitch	y	80
Cut Width	W	4

Governing Equation

Numerical modeling conducted in this research relied on three-dimensional solutions of the governing flow equations system formulation approach. Mass conservation and fluid motion conservation were obtained using the continuity equation (1) together with spatial momentum equations (2), (3), and (4), respectively formulated.

Meanwhile heat transfer between working fluid and twisted tape material was assessed using energy conservation equations applied to fluid domain (5) and solid domain (6) (Bouregueba et al., 2025) within computational thermal analysis framework domain. The k–ω Shear Stress Transport (SST) turbulence model was implemented in this simulation due to its validated ability to resolve intense swirling flow structures and adverse pressure gradients generated by twisted tape inserts effectively in CFD analysis. A key advantage of this model lies in its hybrid formulation, which combines the robust free-stream performance of the k–ε model with the superior near-wall prediction accuracy of the k–ω formulation.Consequently, the k–ω SST model provides a high-fidelity numerical framework for predicting heat transfer enhancement and flow resistance characteristics, thereby allowing more accurate estimation of the Nusselt number and friction factor.

$$\frac{\partial u}{\partial x}+\frac{\partial v}{\partial y}+\frac{\partial w}{\partial z}=0 \tag{1}$$

$$\rho\left(u\frac{\partial u}{\partial x}+v\frac{\partial u}{\partial x}+w\frac{\partial u}{\partial x}\right)=-\frac{\partial p}{\partial x}+\mu\left(\frac{\partial^2 u}{\partial x^2}+\frac{\partial^2 u}{\partial y^2}+\frac{\partial^2 u}{\partial z^2}\right) \tag{2}$$

$$\rho\left(u\frac{\partial v}{\partial y}+v\frac{\partial v}{\partial y}+w\frac{\partial v}{\partial y}\right)=-\frac{\partial p}{\partial y}+\mu\left(\frac{\partial^2 v}{\partial x^2}+\frac{\partial^2 v}{\partial y^2}+\frac{\partial^2 v}{\partial z^2}\right) \tag{3}$$

$$\rho\left(u\frac{\partial w}{\partial z}+v\frac{\partial w}{\partial z}+w\frac{\partial w}{\partial z}\right)=-\frac{\partial p}{\partial z}+\mu\left(\frac{\partial^2 w}{\partial x^2}+\frac{\partial^2 w}{\partial y^2}+\frac{\partial^2 w}{\partial z^2}\right) \tag{4}$$

$$\left(u\frac{\partial T}{\partial x}+v\frac{\partial T}{\partial y}+w\frac{\partial T}{\partial z}\right)=\alpha\left(\frac{\partial^2 T}{\partial x^2}+\frac{\partial^2 T}{\partial y^2}+\frac{\partial^2 T}{\partial z^2}\right) \tag{5}$$

$$\left(\frac{\partial^2 T}{\partial x^2}+\frac{\partial^2 T}{\partial y^2}+\frac{\partial^2 T}{\partial z^2}\right)=0 \tag{6}$$

Data Colection

This study applies various Reynolds numbers to examine flow behavior at different simulation velocities. The Reynolds number, shown in Equation (7), is a dimensionless parameter used to characterize fluid flow conditions. It is determined by fluid density (ρ), average inlet velocity ($\bar{v}$), tube diameter (D), and dynamic viscosity (μ), which together describe the relationship between inertial and viscous forces in the fluid (Faturahman et al., 2026).

$$Re=\frac{\rho.D.\bar{v}}{\mu} \tag{7}$$

The thermo-hydraulic analysis for each twisted-tape variation uses friction factor and Nusselt number values from computational simulations. The Nusselt number (Nu), presented in Equation (8), is a dimensionless parameter representing the ratio of convective to conductive heat transfer at the fluid-solid interface (Roda-Casanova & Fernandes, 2022).

$$Nu=\frac{D.h}{k} \tag{8}$$

The friction factor (f), presented in Equation (9) (Assaf et al., 2025), is a dimensionless parameter representing the magnitude of friction between the working fluid and the tube wall, which causes energy losses and leads to a pressure drop (Δp). Δp denotes the pressure reduction measured in Pa, L represents the heated tube length in m, and D indicates the inner diameter of the tube measured in m.

$$f=\frac{\Delta p}{\left(\frac{L}{D}\right)\left(\frac{\rho.u^2}{2}\right)} \tag{9}$$

The evaluation of the heat exchanger performance is carried out using the Performance Evaluation Criteria (PEC) formula, as shown in Equation (10) (Assaf et al., 2025). PEC is a dimensionless parameter used to evaluate the balance between improved heat transfer and the associated pressure drop losses. In this context, Nu denotes the Nusselt number of the modified heat exchanger, while Nup represents the Nusselt number of the unmodified heat exchanger, specifically a plain tube, which is used as the reference for performance comparison.

$$PEC=\frac{\left({Nu}/{Nu_p}\right)}{\left({f}/{f_p}\right)^{\frac{1}{3}}} \tag{10}$$

Boundary Condition

To accurately represent the heat-exchanger system geometry, an unstructured tetrahedral mesh is used to discretized the domain, which provides high flexibility in resolving intricate surfaces and twisted tape features. The mesh configuration and computational boundaries are presented in Figure 2. Water with 20°C initial temperature was employed as the working fluid when a heat flux of 1200 W/m2 is provided, while Stainless Steel 304 was used as the twisted tape material, with their thermophysical properties summarized in Table 2. For the boundary conditions, a velocity inlet was imposed to define the flow rate corresponding to the specified Reynolds number, whereas a pressure outlet condition was applied at the outlet under atmospheric reference pressure. The pipe wall and twisted tape surfaces were treated using the no-slip wall condition to accurately capture near-wall flow behavior and heat-transfer mechanisms. The simulations were conducted for six Reynolds numbers, namely 6032, 8848, 10618, 12360, 14363, and 16134, to investigate their effects on the thermo-hydraulic performance of the system.

Table 2. Material properties

Material	Density	Thermal Conductivity	Spesific Heat	Dynamic Viscosity
Water	998,2 Kg/m^3	0,6 W/m.K	4182 J/kg.K	0,001003 Kg/m.s
Stainless Steel 304	7954,3 Kg/m^3	14,924 W/m.K	473,62 J/Kg.K	-

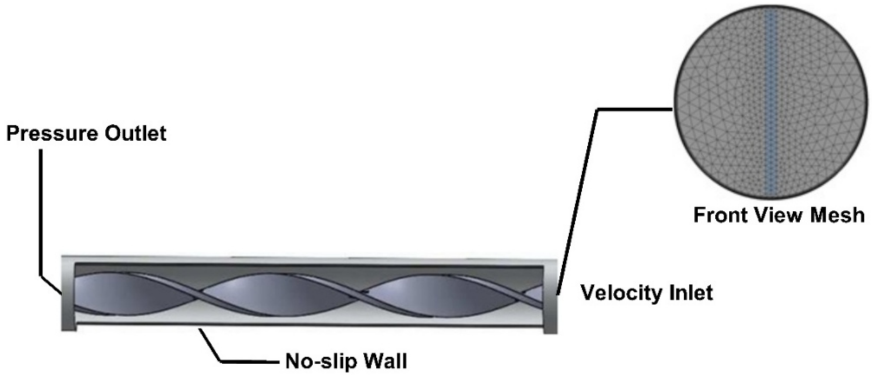

Figure 2. Meshing and boundary of pipe with twisted tape insert

Grid Independence Test

The precision and dependability of CFD analyses are highly influenced by the quality of the computational mesh applied throughout the numerical domain. An unsuitable mesh arrangement can produce considerable discretization inaccuracies and reduce the reliability of thermo-hydraulic predictions. Accordingly, a grid independence assessment was performed to verify that the obtained simulation outcomes remained stable and unaffected by variations in mesh density. In this investigation, three separate mesh arrangements were examined, namely a coarse mesh containing 1.132×10^6 elements, a medium mesh consisting of 2.178×10^6 elements, and a fine mesh comprising 3.38×10^6 elements. The comparison was performed based on the variation of key thermo-hydraulic parameters obtained from each mesh configuration. According to the mesh-independence evaluation summarized in Table 3 and following the method developed by(Roache, 1994), the medium-grid configuration containing 2,178,581 elements was selected as the optimum computational mesh for the present simulation. The selection was based on the Grid Convergence Index (GCI) analysis, which produced an asymptotic convergence ratio approaching unity, indicating that the numerical solution had become sufficiently independent of mesh discretization effects. Furthermore, Figure 3 presents the mesh-sensitivity analysis obtained from the grid independence evaluation.

$$r = \frac{h_1}{h_2} \tag{11}$$

$$p = \frac{ln\left(\frac{f_3 - f_2}{f_2 - f^1}\right)}{ln(r)} \tag{12}$$

$$GCI_{fine} = \frac{f_s|\epsilon_{12}|}{(r^p - 1)} \tag{13}$$

$$GCI_{coarse} = \frac{f_s|\epsilon_{23}|}{(r^p - 1)} \tag{14}$$

$$\frac{GCI_{coarse}}{GCI_{fine} r p} \approx 1 \quad (15)$$

$$\in = \frac{f_{n+1} - f_n}{f_n} \quad (16)$$

Table 3. Mesh independent test result

Mesh Category	Fine	Medium	Coarse
Elements	3,384,255	2,178,581	1,132,043
Nu	114.54	111.81	107.29
r		1.20	
p		2.74	
GCI_{fine}		4.562%	
GCI_{coarse}		7.726%	
GCI Ratio		1.02	
Error	-	2.38%	4.04%

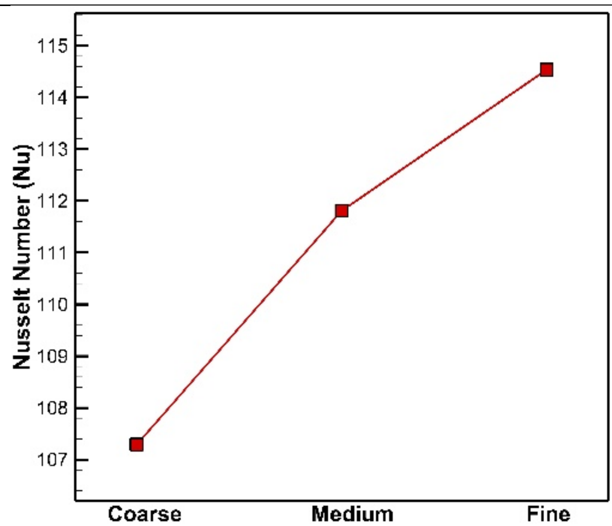

Figure 3. Mesh sensitivity

RESULTS AND DISCUSSION

Validation

Figure 4 presents the validation results of the CFD model through comparisons with experimental data obtained from Dagdevir et al. (Dagdevir & Ozceyhan, 2021) as well as established empirical correlations for both the Nusselt number and friction factor. The computational results show excellent agreement with the experimental measurements and theoretical predictions, indicating the reliability of the numerical model. The governing analytical relationships used for validation are described in Equations (17)-(18). In particular, the Nusselt number is validated using the widely accepted Dittus–Boelter (Seibold et al., 2022), which provide benchmark correlations for convective heat transfer in internal flow, confirming the accuracy of the simulation outcomes.

$$Nu = 0.023 Re^{0.8} Pr^{0.4} \quad (17)$$

Meanwhile, the analytical correlations employed to validate the friction factor include the Blasius equations, as presented in Equation (18) (Liang & Mudawar, 2019), which are commonly used to predict frictional losses in internal flow under different Reynolds number regimes.

$$f = 0.316 Re^{-0.25} \quad (18)$$

Discrepancies remaining under 5% verify that the numerical framework precisely forecasts the thermo-hydraulic behavior of internal turbulent flow. As illustrated in Figure 4(a), a positive correlation exists between the Nusselt number and the Reynolds number. This trend stems from heightened turbulence intensity and a more pronounced disruption of the thermal boundary layer at elevated velocities, which optimizes convective heat transfer via intensified fluid particle mixing within the flow domain. The high alignment among simulated profiles, experimental findings, and the Dittus–Boelter equation verifies the capacity of the CFD model to resolve the underlying thermal mechanisms inside the tube. Conversely, Figure 4(b) reveals a decline in the friction factor as the Reynolds number rises, a phenomenon driven by the diminishing role of viscous forces relative to inertial forces in turbulent regimes. Furthermore, the robust agreement between numerical computations, empirical measurements, and the Blasius correlation indicates that the hydrodynamic trends and pressure drop variations are faithfully reproduced. In conclusion, this validation confirms the stability, precision, and fidelity of the current CFD methodology for evaluating fluid flow and thermal behavior. Consequently, the established model is highly suitable for subsequent thermo-hydraulic exploration of V-cut twisted tape designs across diverse Reynolds numbers to aid industrial thermal system optimization.

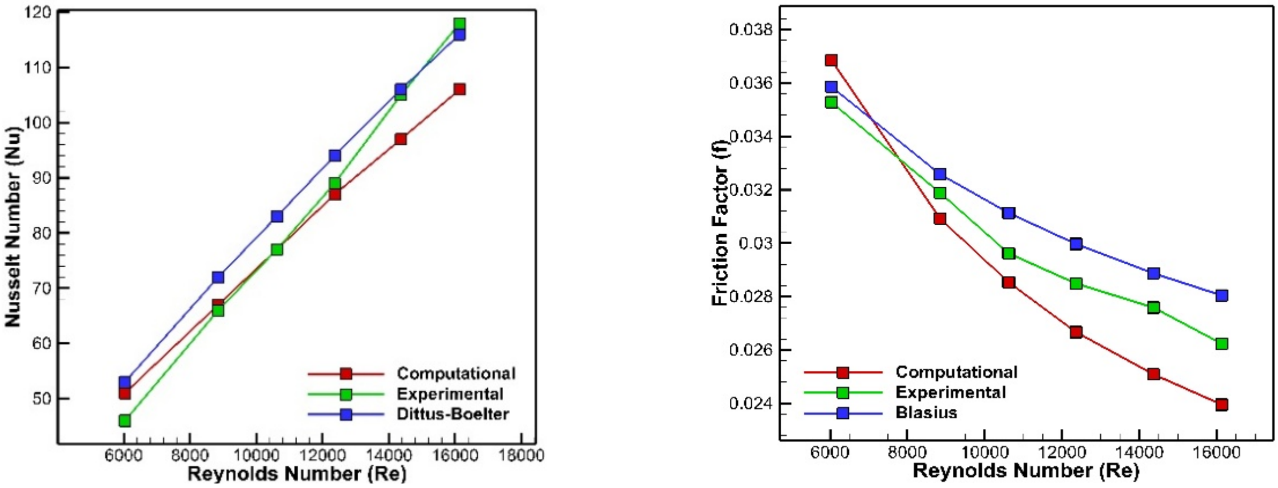

(a) (b)

Figure 4. (a) Nu value validation comparison curve (b) Friction factor value validation comparison curve

Analysis

The interdependence among the Nusselt number, friction factor, and Reynolds number for a baseline smooth tube, conventional twisted tape, and V-cut twisted tape (VTT) inserts across multiple depth ratios is plotted in Figures 5(a) and 5(b). A convergence of structural flow field alterations, intensified turbulence regimes, and surface boundary layer behavior governs the overall thermo-hydraulic efficiency. As illustrated in Figure 5(a), scaling up the Reynolds number yields a continuous growth in the Nusselt number across all investigated models. Physically, higher Reynolds numbers reflect dominant inertial forces and accelerated bulk fluid velocities, which amplify turbulent kinetic energy and momentum dissemination throughout the domain. This fluid movement decreases the thickness of both the thermal and hydrodynamic boundary layers adjacent to the heated perimeter, facilitating a more effective energy exchange between the solid boundary and the moving fluid. Compared to an un-augmented smooth channel, setups incorporating twisted tape components demonstrate remarkably elevated Nusselt numbers due to the generation of rotational swirl paths. The spiral inserts redirect the fluid from a purely stream-wise trajectory into a helical pattern, inducing pronounced tangential velocity components and augmenting radial fluid interactions. This vortex-like action continuously cycles cooler core fluid outward toward the channel surface while concurrently displacing heated peripheral fluid inward. Consequently, thermal stratification is minimized, the periodic redevelopment of the boundary layer is broken down, and convective heat dissipation efficiency is enhanced. However, as documented in Figure 5(b), this advanced thermal behavior comes at the expense of an increased pressure drop. Across all scenarios, the friction factor diminishes as the Reynolds number rises, which matches typical internal turbulent flow dynamics where inertial factors increasingly overpower viscous drag. Even so, traditional tape and VTT systems yield significantly higher friction factors than the smooth tube. The induced rotational flow elongates the actual path of the fluid and escalates wall shear stress by sharpening the velocity gradients near the internal surface. Furthermore, the V-cut design promotes cyclic flow detachment and recirculation cells, increasing internal viscous dissipation. Elevating the depth ratio accentuates vortex intensity and flow blockage, culminating in escalated hydraulic penalties. Thus, while larger depth ratios optimize heat transport via robust mixing actions, they concurrently generate higher flow resistance, underscoring the classic compromise between pressure drop penalties and thermal enhancement in passive un-augmented heat exchanger systems.

Multidisciplinary Output Research For Actual and International Issue (MORFAI Journal) ISSN (e): 2808-6635
Volume 6 No. 5 (2026)

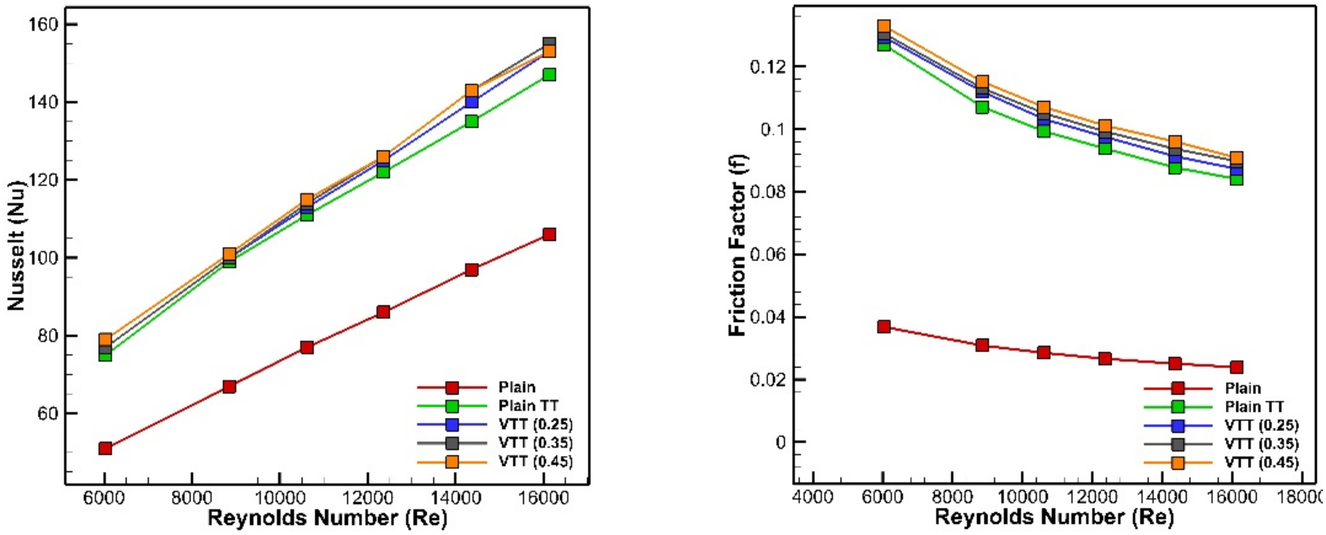

(a) (b)

Figure 5. Variation of Nusselt number (a) and Friction factor (b) with Reynolds number for plain tube, plain twisted tape, and V-cut twisted tape (VTT) configurations with different depth ratios.

Figure 6 illustrates the relationship between the Performance Evaluation Criterion (PEC) and Reynolds number for the plain twisted tape and V-cut twisted tape (VTT) arrangements with several depth-ratio variations. The PEC value indicates the overall thermo-hydraulic behavior by accounting for both heat-transfer improvement and the pressure-drop effect. Consequently, the resulting pattern describes the trade-off between thermal enhancement and hydraulic losses produced by the inserts. Overall, the PEC tends to decrease as the Reynolds number increases for every investigated configuration. Physically, increasing Reynolds number strengthens inertial effects, turbulence intensity, and vortex activity inside the tube. Although these mechanisms improve convective heat transfer through stronger radial mixing and more effective thermal boundary-layer disruption, they also increase wall shear stress and momentum dissipation. At higher Reynolds numbers, the hydraulic penalty tends to increase more significantly, causing the overall PEC to decline. For twisted tape configurations, the enhancement mechanism originates from the swirl flow induced by the insert geometry. The helical flow motion promotes radial transport between the tube core and near-wall regions, continuously renewing the fluid adjacent to the heated surface and improving thermal mixing. However, this swirling motion simultaneously increases the effective flow path length and flow resistance, contributing to higher frictional losses.

The introduction of V-cut geometry further modifies the flow structure through local separation, reattachment, and secondary vortex formation around the cut regions. These secondary vortices intensify turbulence and strengthen radial momentum transport, leading to improved heat-transfer capability compared with the plain twisted tape. The effect of depth ratio demonstrates the importance of balancing these competing mechanisms. Larger depth ratios generate stronger recirculation zones and more intense vortex interaction, which enhance thermal boundary-layer disruption and heat transfer. However, excessive disturbance may amplify friction losses faster than thermal enhancement. Consequently, higher depth-ratio configurations do not necessarily maintain superior PEC values throughout the entire Reynolds-number range. This behavior indicates that an optimum geometric condition is required to maximize thermo-hydraulic effectiveness by achieving sufficient heat-transfer enhancement while limiting hydraulic penalties.

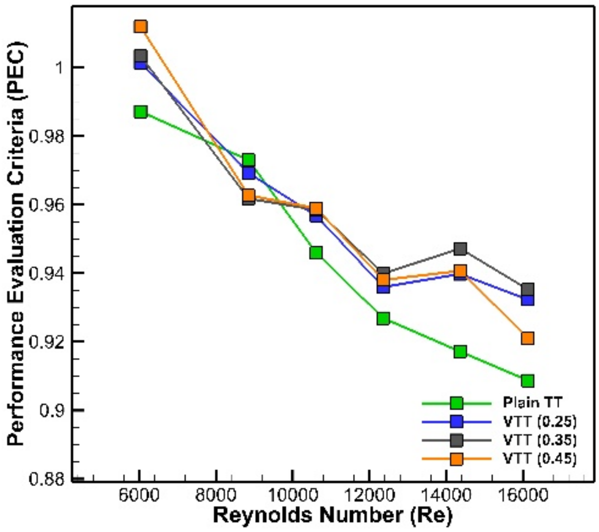

Figure 6. Variation of PEC with Reynolds number for plain twisted tape, and V-cut twisted tape (VTT) configurations with different depth ratios.

Figure 7 presents the velocity contour distribution at the tube cross-section for different insert configurations. In the plain tube configuration, the velocity profile at Re = 12360 exhibits a relatively symmetric distribution with maximum velocity concentrated in the core region and lower velocity near the wall due to the no-slip condition. This behavior indicates predominantly axial flow with limited radial momentum transport, resulting in weaker fluid mixing and a relatively stable near-wall boundary layer. The introduction of the plain twisted tape modifies the velocity field through the generation of swirl flow. The helical motion redistributes momentum across the tube cross-section, enhancing interaction between the core and near-wall regions. This increased radial transport promotes stronger fluid mixing and improves boundary-layer disruption compared with the plain tube. The addition of V-cut geometry further intensifies the flow behavior. For the 0.25 depth ratio, localized disturbance begins to develop around the cut region, producing secondary vortices and moderate velocity redistribution. This configuration improves radial mixing while maintaining relatively controlled flow resistance. Increasing the depth ratio to 0.35 strengthens the flow separation and vortex interaction mechanisms, resulting in more pronounced momentum redistribution and enhanced fluid renewal near the heated wall. Consequently, thermal boundary-layer disruption becomes more effective. Among all investigated cases, the 0.45 depth ratio exhibits the strongest flow disturbance. The deeper cut geometry generates more energetic recirculation zones and stronger secondary vortical structures, leading to intensified radial mixing throughout the tube section. This mechanism is beneficial for convective heat-transfer enhancement because it continuously transports fluid between the wall and core regions. Overall, the progressive modification of the velocity field from the plain tube to the higher-depth-ratio VTT configurations demonstrates the important role of geometry-induced swirl and vortex formation in controlling thermo-hydraulic performance.

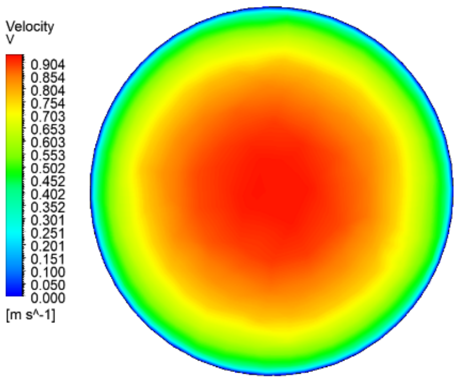

(a)

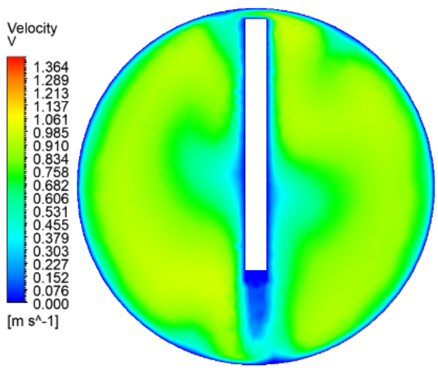

(c)

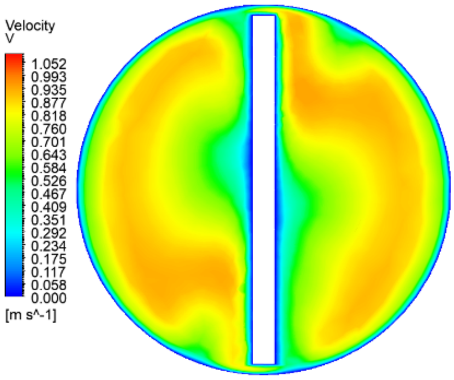

(b)

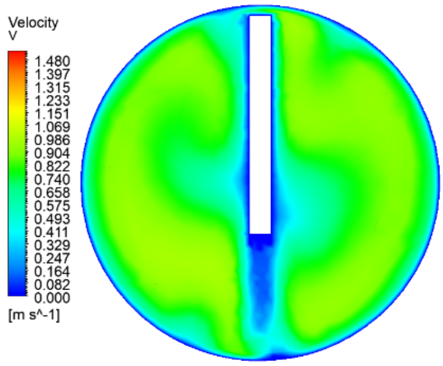

(d)

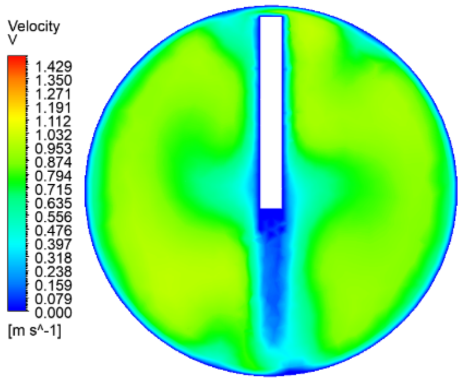

(e)

Figure 7. Velocity contour distribution at the tube cross-section for (a) plain tube, (b) plain twisted tape, and V-cut twisted tape (VTT) configurations with depth ratios of (c) 0.25, (d) 0.35, and (e) 0.45 at Re = 12360.

The impact of varying depth ratios on the cross-sectional thermal fields of plain tubes, conventional twisted tapes (TT), and V-cut twisted tapes (VTT) is visualized in Figure 8. The temperature contours captured at Re = 12360 highlight the role of insert design in driving temperature equalization and fluid mixing. Within the un-augmented plain tube (Figure 8a), the temperature field exhibits a symmetric distribution with negligible lateral shifting. The deficit in convective fluid mixing forces heat transfer to depend primarily on stream-wise advection, enabling a steady thermal boundary layer to form along the internal surface. Consequently, heat transfer between the core fluid and the near-wall region is restricted. This behavior changes with the conventional twisted tape configuration (Figure 8b), which rearranges the thermal profile by inducing swirl flow. The resulting helical flow vectors accelerate the radial transport of thermal energy, strengthening the interaction between the heated fluid near the boundary and the chilled core fluid. As a result, temperature gradients become more redistributed compared with the plain tube, indicating improved thermal mixing and enhanced boundary-layer disruption. For the VTT configuration with a depth ratio of 0.25 (Figure 8c), the V-cut geometry introduces additional flow disturbance that intensifies thermal transport. Secondary vortices generated around the cut regions promote stronger cross-stream mixing, producing a more redistributed temperature field and improved temperature exchange within the tube. As the depth ratio increases to 0.35 (Figure 8d), stronger vortex interaction and recirculation effects enhance radial thermal transport more significantly. The intensified mixing continuously renews fluid adjacent to the heated wall, weakening thermal stratification and improving temperature uniformity across the cross-section. Among all investigated cases, the 0.45 depth ratio configuration (Figure 8e) exhibits the strongest thermal redistribution. The deeper V-cut geometry generates more energetic vortical structures, resulting in highly intensified mixing and more uniform temperature distribution throughout the tube. This behavior indicates more effective convective heat transfer. However, the enhanced thermal performance is also associated with stronger flow disturbance, which contribute to increased hydraulic resistance, consistent with the friction-factor behavior observed previously.

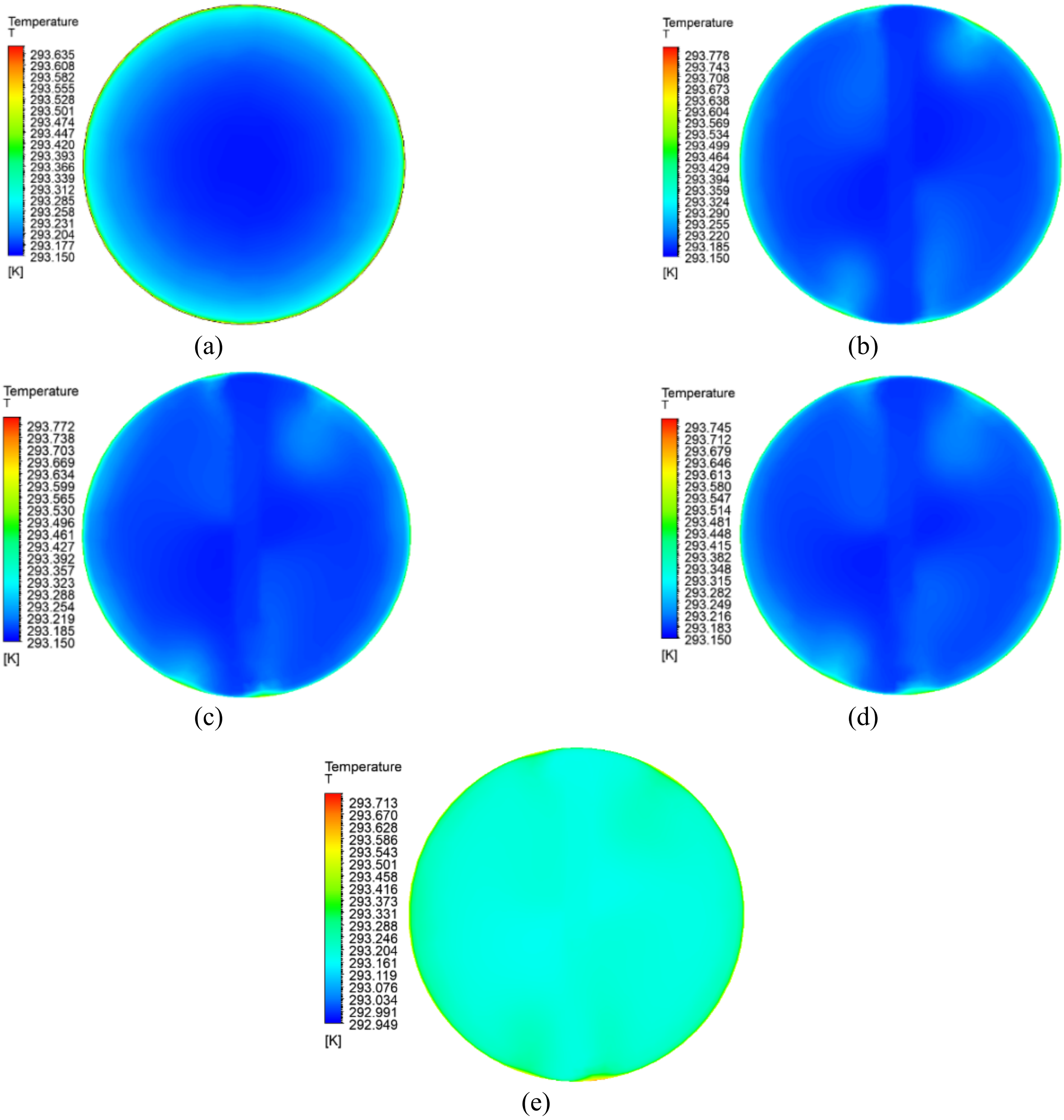

Figure 8. Temperature contour distribution at the tube cross-section for (a) plain tube, (b) plain twisted tape, and V-cut twisted tape (VTT) configurations with depth ratios of (c) 0.25, (d) 0.35, and (e) 0.45 at Re = 12360.

CONCLUSION

A numerical exploration was conducted via CFD analysis to evaluate how changing the depth ratio modifies the thermo-hydraulic characteristics of a tubular heat exchanger fitted with V-cut twisted tape (VTT) elements. Three specific depth ratios ($De/w = 0.25$, 0.35, and 0.45) were systematically examined, focusing on metrics such as internal flow dynamics, friction factor, Nusselt number, and the Performance Evaluation Criterion (PEC). The results indicate that incorporating twisted tape modifications yields a fundamentally restructured internal flow field relative to an unmodified smooth tube. This shift is driven by boundary-layer disruption, heightened radial fluid blending, and swirl induction. Additionally, integrating V-cut geometries accelerates these transport phenomena by generating localized flow recirculation zones, secondary vortex structures, and superior momentum allocation across the entire tube section. The Nusselt number continuously increased as the Reynolds number became higher for all tested cases, whereas the V-cut twisted tape configuration consistently generated greater heat-transfer enhancement than both the plain twisted tape and the smooth tube. A larger depth ratio also intensified vortex formation and flow instability, resulting in stronger thermal mixing and more efficient convective heat-transfer processes within the heat exchanger tube. However, this enhancement was accompanied by higher friction factors due to increased wall shear stress, energy dissipation, and flow obstruction generated by stronger secondary-flow structures.

Assessment of the Performance Evaluation Criterion (PEC) underscores the necessity of balancing thermal dissipation improvements against hydraulic penalties. While increasing the depth ratio boosts heat transport capacity, the accompanying severe flow disturbance can cause pressure drops to outpace thermal benefits. Consequently, overall thermo-hydraulic efficiency depends on a compromise between fluid mixing quality and flow resistance, instead of relying solely on thermal advancement. Visualizations of the velocity and thermal fields corroborate these mechanics, revealing a continuous increase in cross-sectional blending, momentum allocation, and thermal uniformity at higher depth ratios. The most severe vortex interactions and thermal shifts were observed in setups with large depth ratios, verifying that secondary flows driven by insert geometry act as a primary mechanism for regulating thermal transport. In summary, this research confirms that the depth ratio serves as a vital non-dimensional factor shaping the thermo-hydraulic profiles of V-cut twisted tape inserts, offering valuable design guidelines for optimizing passive heat transport augmentations in tubular heat exchangers.

REFERENCES

Assaf, Y., Akroot, A., Alnamasi, K., & Ismail, M. (2025). Investigation Of Heat Transfer Performance In Heat Exchangers Using Hybrid Nanofluids And Twisted Tape Inserts With Fixed Special Rings. *Scientific Reports*, *15*. https://doi.org/10.1038/s41598-025-02135-3

Bouregueba, A., Abdelaziz, B., Rachid, S., & Kherrafi, M. (2025). Heat Transfer Enhancement in a Heat Exchanger Tube Using Twisted Tapes with Circular and Hexagonal Perforations. *International Journal of Thermodynamics*. https://doi.org/10.5541/ijot.1653747

Dagdevir, T., & Ozceyhan, V. (2021). An Experimental Study on Heat Transfer Enhancement and Flow Characteristics of a Tube With Plain, Perforated and Dimpled Twisted Tape Inserts. *International Journal of Thermal Sciences*, *159*(August 2020), 106564. https://doi.org/10.1016/j.ijthermalsci.2020.106564

Diwaker, M. K., & Kumar, A. (2023). Thermo-Hydraulic Performance of Tube Type Heat Exchanger with Semi-Circular Cut Twisted Tape Insert: A Numerical Exploration. *Journal of Heat and Mass Transfer Research*, *10*(1), 159–170. https://doi.org/10.22075/jhmtr.2023.30445.1438

Faturahman, R. A., Waluyo, R., Yuliaji, D., Setiawan, P. H., Maryadi, S. A., Fauzan, M. A., & Juarsa, M. (2026). Analisis Kemampuan Pendinginan Water Cooling Tank (WCT) Berdasarkan Perubahan Daya Heater pada Untai FASSIP-6S. *JTERA (Jurnal Teknologi Rekayasa)*, *10*(2), 159. https://doi.org/10.31544/jtera.v10.i2.2025.159-168

Hasan, S., & Naji, Z. (2023). Augmentation Heat Transfer In A Circular Tube Using Twisted - Tape Inserts: A Review. *Journal of Engineering and Sustainable Development*, *27*, 511–526. https://doi.org/10.31272/jeasd.27.4.8

Hu, Y., & Man, Y. (2023). Energy Consumption And Carbon Emissions Forecasting For Industrial Processes: Status, Challenges And Perspectives. *Renewable and Sustainable Energy Reviews*, *182*, 113405. https://doi.org/https://doi.org/10.1016/j.rser.2023.113405

Kumar, R., Nandan, G., Dwivedi, G., Kumar, A., & Shrivastava, R. (2021). Modeling of Triangular Perforated Twisted Ttape with V-Cuts in Double Pipe Heat Exchanger. *Materials Today: Proceedings*, *46*, 5389–5395. https://doi.org/10.1016/j.matpr.2020.09.038

Liang, G., & Mudawar, I. (2019). Review Of Single-Phase And Two-Phase Nanofluid Heat Transfer In Macro-Channels And Micro-Channels. *International Journal of Heat and Mass Transfer*, *136*, 324–354. https://doi.org/https://doi.org/10.1016/j.ijheatmasstransfer.2019.02.086

Nashee, S. R. (2024). Numerical Simulation of Heat Transfer Enhancement of a Heat Exchanger Tube Fitted with Single and Double-Cut Twisted Tapes. *International Journal of Heat and Technology*, *42*(3), 1003–1010. https://doi.org/10.18280/ijht.420327

Roache, P. J. (1994). Perspective: A Method for Uniform Reporting of Grid Refinement Studies. *Journal of Fluids Engineering*, *116*(3), 405–413. https://doi.org/10.1115/1.2910291

Roda-Casanova, V., & Fernandes, C. M. C. G. (2022). A Comparison Of Analytical Methods To Predict The Bulk Temperature In Polymer Spur Gears. *Mechanism and Machine Theory*, *173*(March), 104849. https://doi.org/10.1016/j.mechmachtheory.2022.104849

Seibold, F., Ligrani, P., & Weigand, B. (2022). Flow and heat transfer in swirl tubes — A review. *International Journal of Heat and Mass Transfer*, *187*, 122455.

https://doi.org/https://doi.org/10.1016/j.ijheatmasstransfer.2021.122455

Singh, S. K., Kacker, R., Chaurasiya, P. K., & Gautam, S. S. (2022). Correlations on heat transfer rate and friction factor of a rectangular toothed v-cut twisted tape exhibiting the combined effects of primary and secondary vortex flows. *International Communications in Heat and Mass Transfer*, *139*, 106503. https://doi.org/10.1016/j.icheatmasstransfer.2022.106503

Sulistiana, A. I., Adinda, A. P., Hakim, B. A., Izza, F. R., & Dianingratri, X. F. (2026). Recovery and Utilization of Waste Heat from Cooler Effluent for Preheating Applications. *Journal of Chemical Engineering Research Progress*, *3*(1), 37–43. https://doi.org/10.9767/jcerp.20597

Thapa, S., Samir, S., Kumar, D.-K., & Singh, S. (2021). A review study on the active methods of heat transfer enhancement in heat exchangers using electroactive and magnetic materials. *Materials Today: Proceedings*, *45*. https://doi.org/10.1016/j.matpr.2021.01.382

Thote, S. A., & Singh, N. P. (2023). Analysis of Friction and Heat Transfer Characteristics of Tubes with Trapezoidal Cut Twisted Tape Inserts. *Fluid Dynamics and Materials Processing*, *19*(3), 711–722. https://doi.org/10.32604/fdmp.2022.021651

Turek, V., Kilkovský, B., Daxner, J., Babička Fialová, D., & Jegla, Z. (2024). Industrial Waste Heat Utilization in the European Union—An Engineering-Centric Review. *Energies*, *17*(9). https://doi.org/10.3390/en17092084